Dynamic Behaviour of Double-Phase-Change Heat-Exchangers

FRANZ MAYINGER and MANFRED SCHULT
Institut für Verfahrenstechnik
der Universität Hannover
Hannover, FRG

ABSTRACT

To predict the dynamic behaviour of a double phase change heat exchanger the thermo- and fluiddynamic effects - especially pressure drop and heat transfer with boiling and condensation - have to be exactly known, which can be achieved by a careful literature study. The system of continuity and constitutive differential equations is not linear and cannot be solved in an analytical way for most cases of applications. Therefore a numerical solution in a computer code is necessary.

For simple geometrical conditions - boiling refrigerant in a tube and condensing water vapour in an annulus around it - measured and theoretically predicted transfer functions are compared and it is shown, that good agreement can be achieved as long as no two-phase flow instabilities occur, the perturbation frequency is not to high and the system pressure is not changed to much. Flow pattern have a strong influence onto the dynamic behaviour. There is a strong coupling between the boiling and condensation side.

Although the dynamic behaviour of the system is not linear, it was possible to evaluate the experimental results by aid of a Fourier analysis and to plot the data in form of transfer functions, demonstrating the amplification coefficient and the phase angle between the perturbated and the corresponding parameter. This analysis can be only performed if the deviation from the linearity is not to large.

1. INTRODUCTION

In power and in chemical engineering frequently heat-exchangers are used, where by condensing saturated vapour on one side liquid of the same or another substance is evaporated. Such an apparatus for heat transport working on both sides with liquid-vapour-mixtures is called a heat-exchanger with double-phase-change. The energy transport in a two-phase flow system has the following advantages.

Even with small temperature differences between the primary and the secondary side of the heat exchanger, an economic heat transport is possible.

The mass flow rate for the energy transport is small due to the large latent heat of evaporization.

Operation is possible also with free convection only because of the large density differences between the phases.

With increasing problems in the world wide energy supply the application of double-phase heat-exchangers may become more and more important especially with safing low temperature energy. In chemical engineering, where aqueous solutions have to be concentrated by partial evaporation using saturated steam as energy supply phase-change has also some benefits if heat has to be transported over long distances. Last not least, low temperature heat can be used in refrigerant processes and in heat pump systems. Also here the primary heat is often available in form of latent heat of evaporization of saturated vapour.

2. FLUID DYNAMIC FUNDAMENTALS

The transient and dynamic behaviour of heat exchangers with single phase flow on both sides was treated in detail in the paper by Shah /1/ and by Schöne /2/. All theoretical models describing the dynamic behaviour of heat exchangers start from the wellknown laws of conservation for mass, energy and momentum.

$$\partial\rho/\partial t + \mathrm{div}\,(\rho\vec{w}) = 0 \tag{1}$$

$$\frac{\partial(\rho h)}{\partial t} + \mathrm{div}\,(\rho h\vec{w}) = \dot{q}\,U_b/A_c \tag{2}$$

$$\frac{\partial(\rho\vec{w})}{\partial t} + \mathrm{div}\,(\rho\vec{w}\vec{w}) = \mathrm{grad}\;p + \eta\,\Delta\vec{w} \tag{3}$$

As shown in the literature the methods describing the dynamic behaviour of single phase heat exchangers are mainly different in the procedure evaluating approximativ solutions for these non linear partial differential equations. With phase change on one side or on both sides additional difficulties in describing the dynamic behaviour arise from a physically correct modelling of the typical two-phase flow phenomena, like slip ratio, pressure drop and heat transfer with boiling and condensation.

Studies of the dynamic behaviour of steam generators - with phase change on one side only - were mainly concerned with controlling and with stability problems. With phase change both phases have to be taken in account in the balance equations

$$\frac{\partial}{\partial z}\left[\rho_F w_F(1-\varepsilon)+\rho_D w_D\varepsilon\right] + \frac{\partial}{\partial t}\left[\rho_F(1-\varepsilon)+\rho_D\varepsilon\right] = 0 \tag{4}$$

$$\frac{\partial}{\partial z}\left[\rho_F w_F h_F(1-\varepsilon)+\rho_D w_D h_D \varepsilon\right]+\frac{\partial}{\partial t}\left[\rho_F h_F(1-\varepsilon)+\rho_D h_D \varepsilon\right]=\dot{q} U_b/A_c \tag{5}$$

$$\frac{\partial}{\partial z}\left[\rho_F w_F{}^2(1-\varepsilon)+\rho_D w_D{}^2 \varepsilon\right]+\frac{\partial}{\partial t}\left[\rho_F w_F(1-\varepsilon)+\rho_D w_D \varepsilon\right]=$$

$$=\frac{\partial p}{\partial z}-R_{diss}-g\left[\rho_F(1-\varepsilon)+\rho_D \varepsilon\right]; \tag{6}$$

which involves a number of additional unknown variables. Profos /3/ developed a theoretical model for calculating the dynamic behaviour of the outlet conditions in a steam generator assuming that the heat flux is independed from the pipe-wall temperature. In continuing this work Isermann /4/ incorporated the coupling between pipe-wall temperature and heat transfer to the pipe. Hasenkopf /5/ additionally regarded the coupling of the fluid temperature and the gas temperature on the combustion side of a boiler. Numerical integration of the differential equations instead of looking for analytical solutions by using linearization methods has the advantage that local alterations of the thermodynamic conditions can be taken better in account /6, 7/. The geometrical extension of the heat exchanger or of the steam generator, however, has then to be nodalized in a proper way and the difference between the numerical solution and the real condition becomes smaller with a more detailed subdivision of the flow channel.

With double phase change a number of special two phase flow peculiarities arise which do not exist in single phase flow. With phase change various flow pattern can occur which have consequences with respect to heat transfer and pressure drop. Changes in mass flow rate, pressure and temperature may cause flow instabilities in a boiling channel. Bergles /8/ gave a detailed classification of all possible appearances of these instabilities. He distinguishes mainly between a static and a dynamic instability. Static instability results in a new steady state condition, whereas dynamic instabilities produce a periodical change in the flow around the old or a new mean value.

For dynamic instabilities usually more than one mechanism is responsible. The two main origins for dynamic instabilities are density waves and pressure drop changes. The later ones mainly occur in fluid dynamic systems, filled with compressible volumes /9/.

A theoretical model was developed and experiments were performed by Schult /1o/ researching the dynamic behaviour of double phase change heat exchangers. The theoretical model starts from the conservation laws (equations 4 - 6) and is coupling both sides of the heat exchanger - the condensing and the evaporating one - via the heat fluxes transported and the heat stored. In the model coaxial flow of both substances in a tube and in an annulus is assumed with vapour condensing in the annulus, as illustrated in fig. 1.

In order, not to overstress the mathematical treatment and to stay within economical computer times, the model contains the following simplifications:

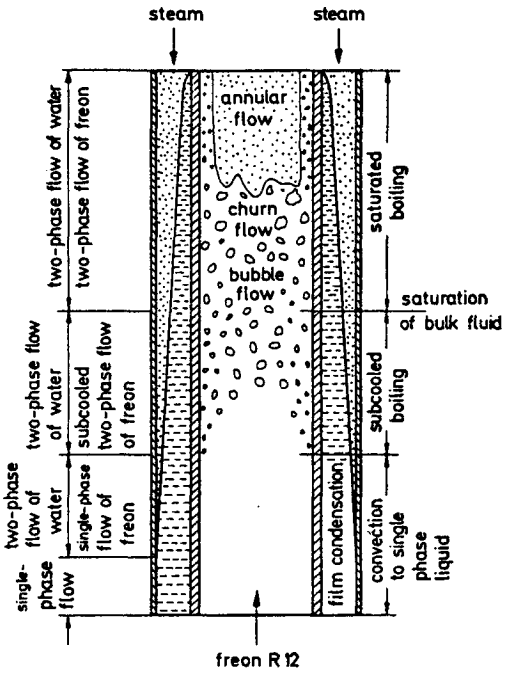

Fig. 1: Flow regions of the vapour transformer

The flow on each side of the heat exchanging wall is one-dimensional

Vapour and liquid are in thermodynamic equilibrium

The temperature of the solid wall is only a function of the length and of the time, i.e. it is assumed that the wall is very thin or has very high heat conductivity.

On the boiling side the fluid enters the channel sub-cooled and

on the condensing side the vapour is saturated.

There is no special assumption for the flow patterns on the boiling side, however, on the condensing side falling film-flow of the liquid is regarded to be present. The coupling conditions, between the condensing and the boiling side, can be easily derived with the help of fig. 2, illustrating a volumetric unit of this single tube annular heat exchanger. The energy balance for the inner tube - boiling side - reads

$$\dot{Q}_{sp} = \dot{Q}_{ax} + \dot{Q}_{w} - \dot{Q}_{f} \qquad (7)$$

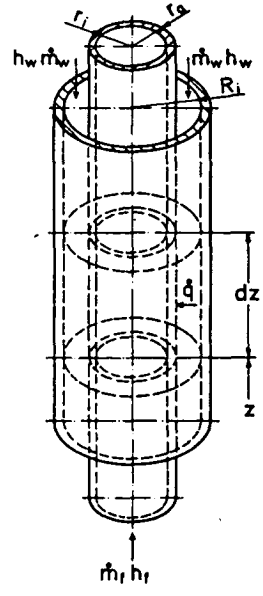

Fig. 2: Volume element of the test section

where the various heat fluxes are defined as follows:

$$\dot{Q}_{sp} = m_R \cdot c_p \cdot \partial \vartheta_R / \partial t \,, \tag{8}$$

$$\dot{Q}_w = \alpha_w U_{wb} (\vartheta_w - \vartheta_R) dz \,, \tag{9}$$

$$\dot{Q}_f = \alpha_f U_{fb} (\vartheta_R - \vartheta_f) dz \,, \tag{10}$$

$$\dot{Q}_{ax} = \lambda A_R (\partial^2 \vartheta / \partial z^2) dz \,. \tag{11}$$

The axial heat flux $\dot{Q}_{ax}$ is small compared with the heat fluxes $\dot{Q}_w$ and $\dot{Q}_f$ in radial direction, due to the fact that the heat transfer coefficients on the side of condensation and of evaporation are very high. With negligible axial temperature gradient $d\vartheta/dz$ in the wall, the wall temperature at the elevation z and at the time t_1 reads

$$\vartheta_{R_1} = \vartheta_{R_o} \left[1 + e^{-\left(\frac{1}{\tau_w} + \frac{1}{\tau_f}\right)\Delta t} \right] \tag{12}$$

In equation 12, the ratio of the heat capacity versus the heat added or subtracted are expressed in the form of the time constants τ_w and τ_f

$$\tau_w = \frac{m_R \cdot c_R}{\alpha_w A_{wb}} \tag{13}$$

$$\tau_f = \frac{m_R \cdot c_R}{\alpha_f \cdot A_{fb}} \tag{14}$$

The heat transfer coefficients α_w and α_f are functions of the fluid-dynamic and thermodynamic conditions on both sides of the heat exchanging wall. For solving the system of differential equations (equation 4 - 6) together with the radial energy balance, constitutive equations have to be developed describing the following physical phenomena

subcooled boiling on the evaporating side

two-phase flow pressure drop on the evaporating and on the condensing side

slip ratio on the evaporating and on the condensing side

heat transfer with boiling and with condensation.

Most informations for describing these phenomena can be taken from the literature in form of empirical equations. However, one has to be very careful to select these equations in such a way that they meet the real conditions as good as possible.

2.1 Subcooled Boiling

With high heat flux densities vapour bubbles are formed at the wall though the mean temperature of the fluid is below the saturation temperature. This phenomenon, called subcooled boiling, improves the heat transfer coef-

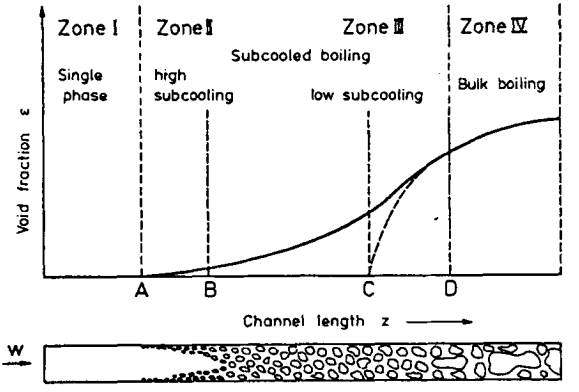

Fig. 3: Vapour void fraction along the length of a heated channel

ficient considerably. 4 axial zones are distinguished with subcooled boiling as demonstrated in fig. 3. In zone I the heat is transported from the wall to the fluid by single phase forced convection. By heat addition along the channel the temperature of the wall and of the fluid is increased. In zone II the first vapour nuclei are formed and the evaporation is still increasing in zone III. Finally in zone IV, the mean temperature of the liquid reaches the saturation temperature corresponding to the pressure being present at this elevation. There is a number of papers in the literature, describing the phenomena with subcooled boiling. Reference is only made to a few of them /11 - 14/.

In the model of Schult /10/ it is assumed that up to the position B in fig. 3, where the vapour void rises considerably, the heat transfer is governed by single phase flow and down stream from this point, heat transfer correlations for fully developed boiling were used. The position for this sudden change in the heat transfer coefficient was correlated using the theory of Saha and Zuber /12/ and of Onal /15/. Both theories are valid for a variety of liquid substances.

2.2 Friction Pressure Drop

In the literature there is a large number of papers dealing with two-phase flow friction pressure drop. For the boiling side, the Baroczy-Chisholm equation /16/ gave best results compared to calibration tests performed in an experimental facility, discussed later. The Baroczy-Chisholm equation gives the ratio between the two-phase flow friction pressure drop and the friction pressure drop if the liquid part would flow only in the channel.

$$\frac{\Delta p_{2Ph}}{\Delta p_{Fo}} = 1 + (\Gamma^2 - 1)\left[B\dot{x}^{0,9}(1-\dot{x})^{0,9} + \dot{x}^{1,8}\right] \qquad (15)$$

This equation contains a term for the density and the viscosity ratio

$$\Gamma = (\rho_F/\rho_D)^{0,5}(\eta_D/\eta_F)^{0,125} \qquad (16)$$

and the constant B can be taken from tab. 1. Equation 15 contains the local quality $\dot{x}$ which continueously changes along the boiling channel.

Tab. 1: Values of B for smooth tubes

Γ	$\dot{m}$ (kg//m²s)	B
≤ 9,5	≤ 500	4,8
	500 < $\dot{m}$ < 1900	2400/$\dot{m}$
	≥ 1900	55/$\dot{m}^{1/2}$
	≤ 600	520/ ($\dot{m}^{1/2}$)
9,5 < Γ 28	> 600	21/Γ
≥ 28		15000/ ($\Gamma^2\dot{m}^{1/2}$)

In the literature the friction pressure drop in a condensing vapour flow usually is treated as a single phase gas flow, however, taking in account that the volumetric mass flow rate is decreasing due to the condensation effect. This method is certainly correct as long as the condensed liquid film is thin compared to the cross flow area of the vapour. In double phase change heat exchangers usually all vapour is condensed and then the friction pressure losses have to be calculated in a similar way as usual for two-phase flow, i.e. with a two-phase friction multiplier. For detailed information reference is made to the thesis by Schult /10/.

2.3 Slip Ratio

For boiling flow as a good prediction of the slip ratio s between the phases

$$s = \frac{w_D}{w_F} \tag{17}$$

the correlation by Nabizadeh /17/ can be used, which is based on the theory by Zuber and Findlay /18/. Nabizadeh is not directly giving a correlation for the slip ratio s but for the volumetric void fraction ε is correlated with the slip ratio s via

$$s = \frac{\dot{x}}{1-\dot{x}} \cdot \frac{1-\varepsilon}{\varepsilon} \cdot \frac{\rho_F}{\rho_D} \tag{18}$$

Using Zuber/Findlay's theory, the mean void fraction $\bar{\varepsilon}$ reads

$$\bar{\varepsilon} = \frac{\dot{x}}{\rho_D}\left[C_o\left(\frac{\dot{x}}{\rho_D}+\frac{1-\dot{x}}{\rho_F}\right)+\frac{1{,}18}{\dot{m}}\left(\frac{\sigma_g(\rho_F-\rho_D)}{\rho_F^2}\right)^{0{,}25}\right]^{-1} \tag{19}$$

where the factor C_o is given by Nabizadeh as:

$$C_o = \dot{\varepsilon}\left[1+\frac{1}{n}+Fr_o^{-0{,}1}\left(\frac{\rho_D}{\rho_F}\right)^n\left(\frac{1-\dot{x}}{\dot{x}}\right)^{1{,}22n}\right] \tag{20}$$

with

$$n = \sqrt{0{,}6\,\frac{\rho_F-\rho_D}{\rho_F}} \tag{21}$$

and

$$Fr_0 = \dot{m}^2/(\rho_F^2 g d)$$

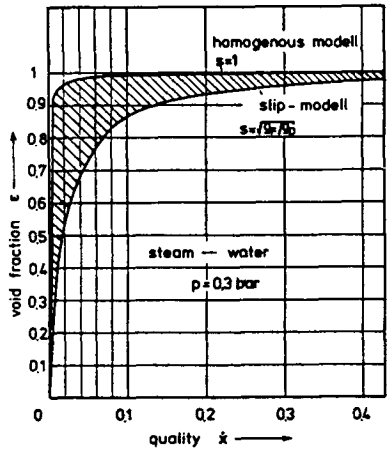

Fig. 4: Void pre-slip model, dicted by slip model and with homogeneous flow

Principally the theory by Zuber and Findlay modified by Nabizadeh, can also be used for the condensing vapour flow. For these parts of the condensing channels where the quality is larger than 0,3, there is almost no or a negligible difference in the prediction of the void fraction by using a slip model or a homogeneous model with identical velocities of vapour and liquid, as demonstrated in fig. 4. Therefore with a good approximation homogeneous flow can be assumed on the condensing side.

2.4 Heat Transfer

The local heat transfer with condensing is dependent whether the falling film flow is laminar or turbulent. Correlations in the literature differ sometimes widely even for identical fluid dynamic and thermodynamic conditions as illustrated in fig. 5. Best agreement with measured values was found for laminar film flow using Hewitt's /19/ equation and for turbulent condition with Kosky /20/ equation.

With boiling two regions of heat transfer mechanism have to be distinguished as wellknown in the literature. In the first one, nucleate boiling with bubbles formed at the heated wall prevails and in the second one an only thin liquid film is present at the wall evaporating at its surface. For the film evaporation an equation given by Ahrens /21/

$$\frac{\alpha_{2Ph}}{\alpha_{Fo}} = C_3\left[B_o \cdot 10^{-4} + C_4 (1/X_{tt})^r\right](1+d_i/L)^s$$

$$C_3 = 0{,}85 \qquad C_4 = 4{,}5 \qquad r = 0{,}35 \qquad (22)$$

$$s = (1/X_{tt})^t \qquad t = 0{,}41$$

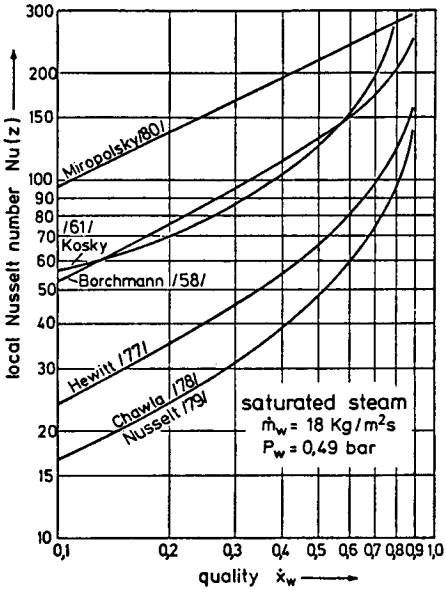

Fig. 5: Local Nusselt numbers for condensing steam as predicted by different authors

$$X_{tt} = \left(\frac{\rho_D}{\rho_F}\right)^{0,5} \left(\frac{\eta_F}{\eta_D}\right)^{0,1} \cdot \left(\frac{1-\dot{x}}{\dot{x}}\right)^{0,9} \qquad (22)$$

can be used. Equation (22) in its principal form is wellknown from the literature.

From the numerous correlations predicting heat transfer with bubble boiling under free and forced convective conditions, the equation by Lavin /22/

$$\dot{q} = 0,25 \frac{\lambda_F}{d_a}\left[\frac{d_a^2}{\eta_F d_i}\right]^{0,69} \cdot Pr^{0,69}\left[\frac{\rho_F}{\rho_D} - 1\right]^{0,31}\left[\frac{p\, d_a}{\sigma}\right]^{0,31} \cdot \dot{q}^{0,69} \qquad (23)$$

gave best agreement with the measurements.

Under certain conditions especially if the temperature difference between the condensing vapour and the boiling liquid is large, critical heat flux conditions may arise with a consequent sudden change in the heat transfer coefficient. There are several equations in the literature /10/ predicting the boiling crisis.

3. EXPERIMENTAL SET UP

The above mentioned balance equations and constitutive correlations were combined in a computer program to predict the dynamic behaviour of a heat exchanger with phase change on both sides. A pure theoretical treatment without experimental assessment could give results far away from the real behaviour of the nature. Already the selection of equations describing single phenomena and separate effects, like heat transfer with boiling and condensation or two-phase pressure drop needs some calibration tests to find a correlation best fitted to the geometrical and fluid dynamic conditions in the heat exchanger. The computer code therefore was tested in an experimental program, which was performed in a test rig with a very simple double phase change heat exchanger, consisting only of two vertical concentric tubes, where in the inner one, under up-flow conditions, the refrigerant R 12 was evaporated and in the annulus, between the inner and the outer tube, under downflow conditions, water vapour was condensed.

The design of the annular test section with the main measuring devices, is shown in fig. 6. On both sides of this simple heat exchanger, the mass flow rate, the pressure and the temperature were measured at the inlet as

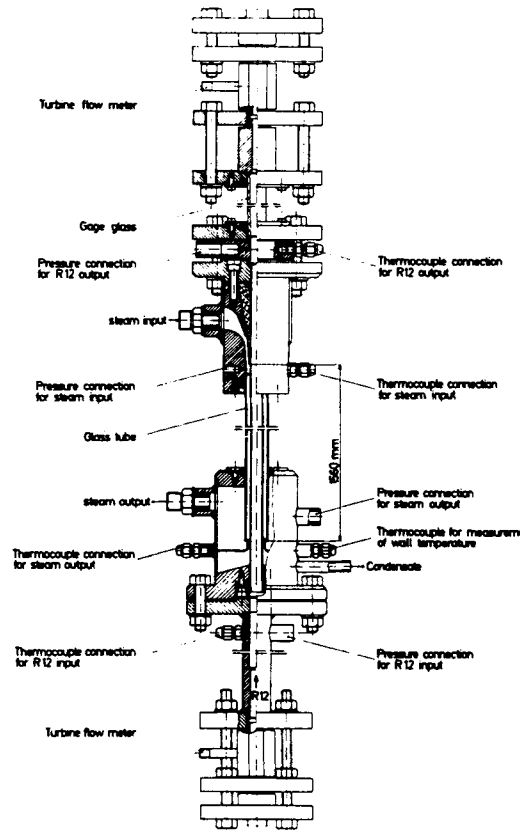

Fig. 6: The double-pipe evaporator - test object

well as at the outlet. The pressure was picked up by electrical pressure gauges and the temperature was determined by thermocouples. Much care was taken to get correct readings of the mass flow rate changes. It pointed out, that turbine mass flow meters were the best sensors for single phase flow as well as for two phase flow. For the later conditions a special calibration procedure combined with a theoretical treatment is necessary to get correct results /23/. In single phase flow the turbine impeller is mainly driven by the momentum of the flow, while the shear stress and consequently the friction on the turbine vanes may be neglected. For a two-phase flow the momenta of vapour and liquid have to be added to a total momentum including the rotation of the turbine wheel. Liquid and vapour in a two-phase flow have different velocities and usually also a large difference in density. Therefore the quality and the void fraction have to be known. The void fraction was measured by the γ ray attenuation method. For the dynamic measurements the intensity of the γ source had to be high enough to get correct readings also for oscillations with high frequency. A 2 Curie γ source therefore was used.

The double phase change heat exchanger was incorporated in a test rig consisting of 2 loops as demonstrated in fig. 7. One of the loops provides the saturated water vapour condensing in the test section, and the other one, the liquid refrigerant evaporating in the heat exchanger.

The refrigerant is only partially evaporated in the heat exchanger, which consists on both sides of stainless steel. The pump 1 delivers liquid refrigerant to the test section 6. The two-phase mixture produced there, is condensed and subcooled in the condenser 9, and from there, the refrigerant flows back to the pump 1. On the condensing side of the test section - the annular heat exchanger - saturated steam of 25 bar, produced in a steam generator 14, is reduced to the test conditions by means of a diaphragm valve 1 By this reduction in pressure the steam becomes superheated and it has therefore to be cooled down to saturation temperature. This is performed in the injection cooler 16.

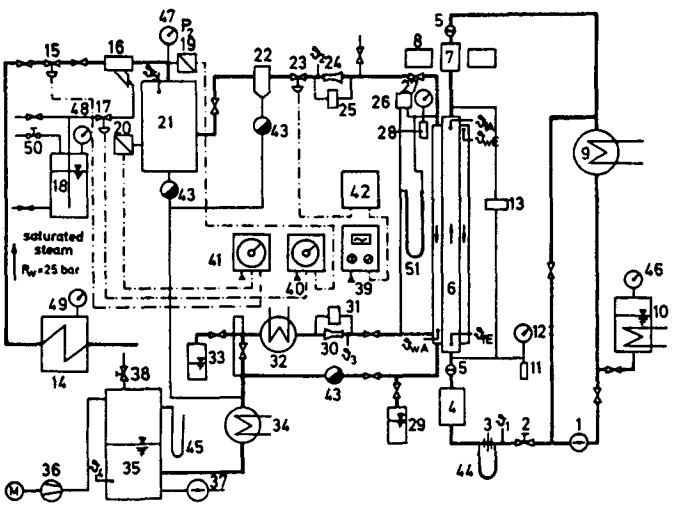

Fig. 7: Schematic of the coupled water-loop and freon R 12-loop

Sinusoidal perturbations can be imposed onto the mass flow rate of the steam and of the refrigerant at the inlet of each side to the test section. A PI-controller 24, is used for mass flow rate control. It receives its nominal value from a pneumatic sinus transmitter, and its actual value from a differential pressure sensor, which in this case can be either a venturi tube or a turbine flow meter. The signal of the command variable is transmitted to a diaphragm valve. Due to the fact that not all of the steam entering the test sections is always condensed a two-phase mixture may leave the test section and therefore liquid and vapour is separated to measure each flow rate separately in addition.

4. THEORETICAL AND EXPERIMENTAL RESULTS

The influence of the various flow pattern and of the different heat transfer mechanisms onto the energy transport between condensing steam and evaporating refrigerant, were tested under steadystate conditions at the beginning. This was not only necessary for calibrating the measuring technique and for selecting the equations describing the physical phenomena test, but also for getting a better understanding of the dynamic effects observed later. In fig. 8 the courses of temperature, heat transfer coefficient and heat flux density along the test section, are demonstrated. In this test the water vapour was condensed only partially, so that with neglecting the small pressure drop, the temperature staid constant anlong the whole test section.

The refrigerant R 12 enters the heat exchanger subcooled and undergoes after a certain distance from the inlet position subcooled boiling. In the example, shown in fig. 8, the refrigerant reaches saturation temperature after approximately flowing half the way of the test section. From this position on the temperature of the refrigerant slightly decreases due to the pressure drop in the tube. The heat flux density $\dot{q}$ is governed by the temperature difference between the condensing steam ϑ_w and the evaporating refrigerant ϑ_f. This temperature difference decreases continuously in the first half of the test section and from thereon it slightly increases.

The heat transfer coefficient α_w on the steam side, is mainly depending from the thickness of the water film on the wall and from the flow con-

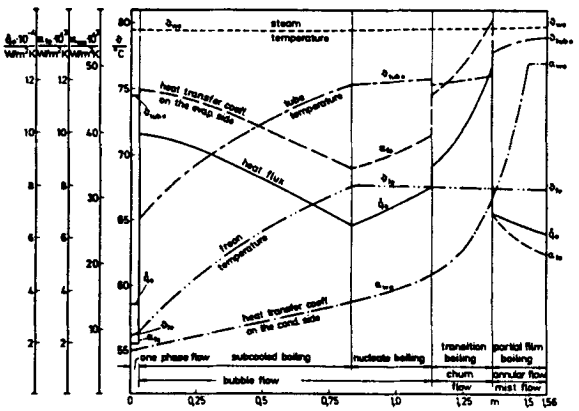

Fig. 8: Steady-state results of a caldulated vapour transformer

ditions- laminar or turbulent -. In the upperpart of the heat exchanger - right side of fig. 8 - the liquid film is thin and the heat transfer coefficient therefore high.

The heat flux density $\dot{q}$ is slightly diminuated in the region of subcooled boiling, because the temperature difference between steam and refrigerant becomes smaller. The heat transfer coefficient α_f on the evaporation side and the heat flux density $\dot{q}$ are mainly coupled in the region of bubble boiling, because α_f is a function of the heat flux density there.

When saturation temperature is reached in the refrigerant, the heat flux density increases, because the temperature difference between the tube wall and the fluid, as well as the heat transfer coefficient on the steam side are rising. This effect is supported by the pressure drop on the refrigerant side. The bubble boiling is followed by two-phase flow heat transfer - surface evaporation - and the heat flux is still increased by a slight improvement of the heat transfer coefficient on the refrigerant side. This is due to the fact that the velocity of the two-phase flow is increased by vapour production.

In the example, shown in fig. 8, boiling crisis occured in the upper part of the test section. This is demonstrated by the sudden deterioration of the heat transfer coefficient α_f on the boiling side. Consequently also the heat flux density $\dot{q}$ is decreasing.

The data measured in the dynamic tests were evaluated by using the Fourier analysis. The perturbations were always sinusoidal, however, the responding functions did not have exactly sinusoidal character, but were somewhat distorted, as demonstrated in fig. 9. This is due to the nonlinear behaviour of the heat exchanger. So the question rises, how the dynamic behaviour can be presented in a simple graphical way. Evaluating the experiments, it pointed out, that the measured data could be represented by super imposing the basic oscillation of the frequency ω with the first harmonic of the frequency 2ω. So the basic oscillation can be presented as a transfer function. The absolute value of the transfer function can be

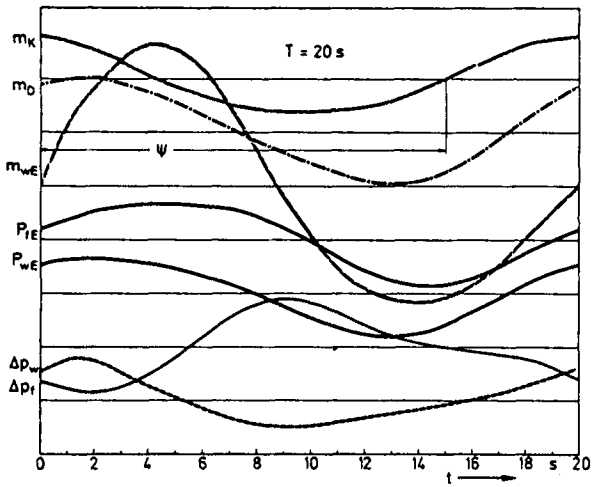

Fig. 9: Temporal course of fluiddynamic parameters corresponding sinusoidal perturbances

written in dimensionaless form

and is called the amplification coefficient. Y_0 and X_0 are steadystate values. Y is the amplitude of the response function and X is the amplitude of the disturbance function. In addition a phase angle ψ can be defined. It is determined from the difference between the two zero passages of the disturbing oscillation and the response oscillation. When the oscillation of the response lags behind the disturbance oscillation, the phase angle is defined as positiv.

There are three main classes of perturbations possible in a double phase change heat exchanger, namely perturbations of

mass flow rate
temperature and
pressure.

Principally these perturbations can occur on both sides of the heat exchanger, however, on the condensing side temperature changes are always strictly linked with pressure variations, because of the saturation conditions in the steam atmosphere. Pressure changes usually are not regarded as normal operation transients and their modelling needs additional correlations for physical phenomena, like propagation effects of pressure waves, not described here, and not incorporated in the above mentioned computer code. Therefore the discussion will be concentrated to oscillations and perturbations of mass flow rate and temperature.

Discussing the consequences of perturbations one has strictly to distinguish whether the transient behaviour is stable or whether instabilities - for example due to boiling crisis or pressure drop effects - occur. In stable behaviour the system is adjusted to a new quasi steadystate around which the thermo- and fluiddynamic status is oscillating. Instabilities show a very rapid and strong change in the fluiddynamic conditions and the oscillations are not quasi steady.

4.1 Perturbations On The Primary Side

The condensing steam on the primary side is saturated and therefore temperature fluctuations would be necessarily linked with pressure changes. The deliberations on the dynamic behaviour under normal operation transients therefore can be concentrated to mass flow rate perturbations on the primary side. The correlations discussed in chapter 2, do not fully take in account instability effects, especially if they are consequences of sudden changes in the flow pattern. Therefore deviations between measured and theoretically predicted values were mainly observed in connection with flow pattern changes.

Best agreement between theory and experiment was found with smaller frequences of the perturbations, which easily can be understood remembering the assumptions in the theoretical model which neglected the heat stored in the tube walls. In fig. 10 the transfer function and the shift of the phase angle is demonstrated for the mass flow rate $\dot{m}_D$ of the vapour produced by

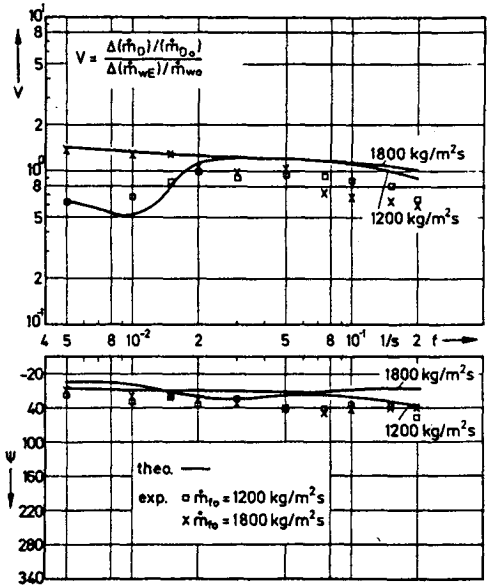

Fig. 10: Transfer functions of the vapour mass flow at the exit of the evaporating side.
Comparison between the calculated and measured data.

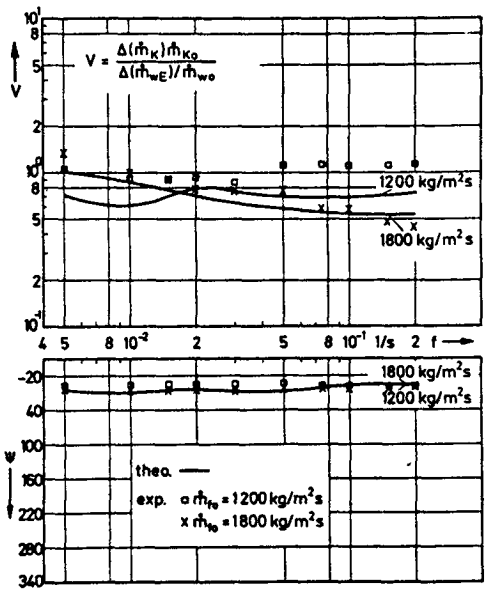

Fig. 11: Transfer functions of the condensate mass flow at the exit of the condensing side. Comparison between the calculated and measured data.

evaporation of the refrigerant. The mass flow rate $\dot{m}_{wo}$ of the water vapour, before the oscillations started was 18 kg/m²s and the perturbations in this mass flow rate $\Delta(\dot{m}_{wo})$ at the inlet of the test section, imposed later on, were 6,5 kg/m²s. The steadystate mass flow rates on the refrigerant side $\dot{m}_{fo}$ were 1.800 kg/m²s and 1.200 kg/m²s respectively. In the figure the amplification coefficient and the phase angle is plotted. Deviation between measurement and experiment are mainly in regions where instabilities were observed.

In fig. 11 the transfer functions for the mass flow rate of the condensed water vapour $\dot{m}_K$ is illustrated.

In the correlations discussed in chapter 2 it is assumed that on both sides of the heat exchanger vapour and liquid are in thermodynamic equilibrium. This is not fully the case in reality because the liquid boundary layer on the boiling side is superheated and the liquid film of the condensed water on the other side is slightly subcooled. With periodic changes of the temperature in these boundary layers effects of heat storage occur influencing the amplification coefficient and the phase angle on the refrigerant side as well as on the water vapour side.

From the fig. 10 and 11 it can be seen that at low perturbation frequences the agreement between theory and experiment is better than at the higher ones. With increasing frequency the damping effects of the fluid boundary layers on both sides of the heat exchanger gain more influence. These damping effects are reducing the maxima and the minima of the amplification coefficient, which are therefore overpredicted in the theory compared to the experiment.

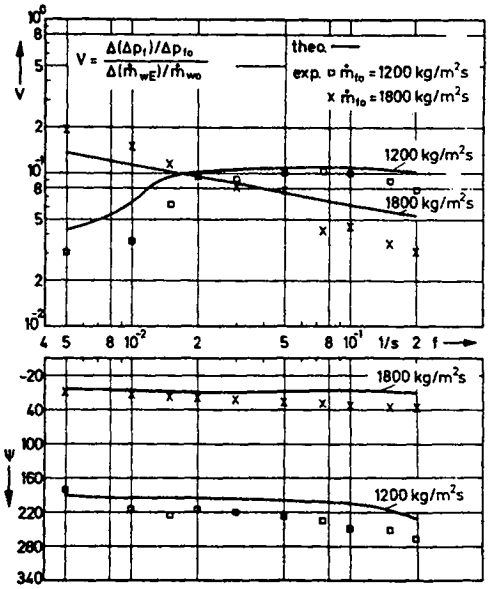

Fig. 12: Transfer functions of the pressure drop on the evaporating side. Comparison between the calculated and measured data.

The pressure drop is more sensitiv to perturbations than the mass flow rate. On the evaporation side as demonstrated in fig. 12, the agreement between calculated and measured values is still not to bad. However, on the condensing side there are large quantitative discrepances although qualitatively there is agreement in the tendency of the amplification coefficients versus frequency, as shown in fig. 13. These discrepances can be explained by the different components contributing to the pressure drop on the condensing side. The total pressure drop on this side is mainly influenced by friction and momentum change. Both have opposit signs because the decreasing momentum due to condensing vapour results in a pressure increase and friction is always reducing the pressure. Under certain conditions both terms may be of the same order and then the pressure change is almost zero. As long as there is no stagnant liquid water in the annulus of the condensing side, the potential term has no influence because the gravity force is in equilibrium with the wall friction of the liquid falling film flow. The amplification coefficient is related to the steadystate value and therefore with almost zero steadystate pressure drop a very small mistake in predicting the steadystate conditions gives large errors in the transfer functions. As shown in fig. 13, the amplification factor for the pressure drop in the condensing flow can be in the order of ten.

In the fig. 10 - 13 the transfer functions were always related to a steadystate mass flow rate.

The theoretical model, however, is not restricted to certain fluiddynamic or thermodynamic states. It can be used in a wide range of mass flow rates, pressures and temperatures, as shown in the fig. 14 and 15. In both fig. as the previous ones, the mass flow rate of the saturated vapour entering the annulus and condensing there, was perturbated. Instead of constant mass flow rates of the refrigerant, now constant pressure (fig. 14) and constant subcooling (fig. 15) on the evaporating side - i.e. at the entrance of the re-

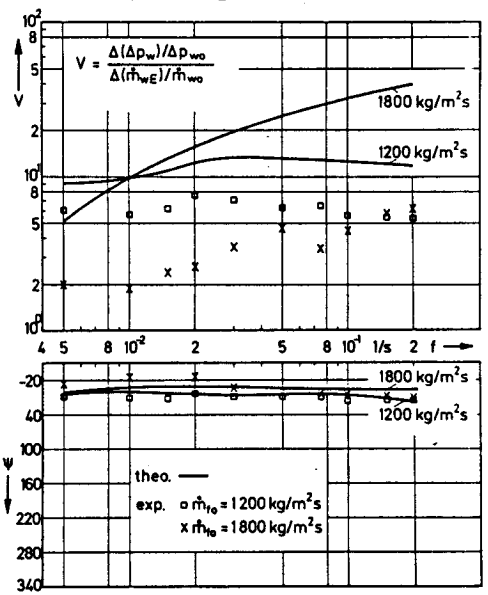

Fig. 13: Transfer functions of the pressure drop on the condensing side. Comparison between the calculated and measured data.

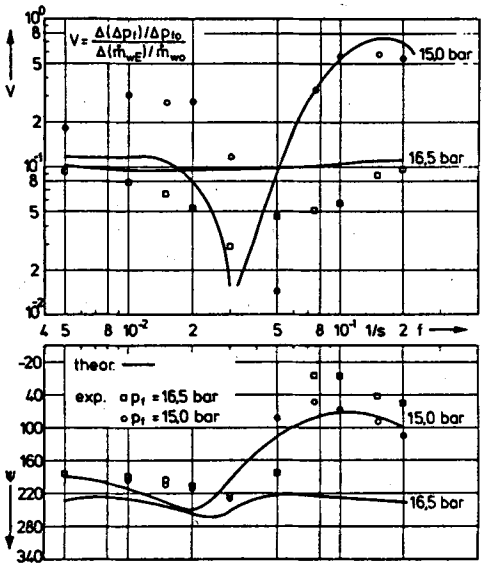

Fig. 14: Amplification factor and phase shift measured and calculated for pressure drop on boiling side. Mass flow rate of condensing vapour perturbated.

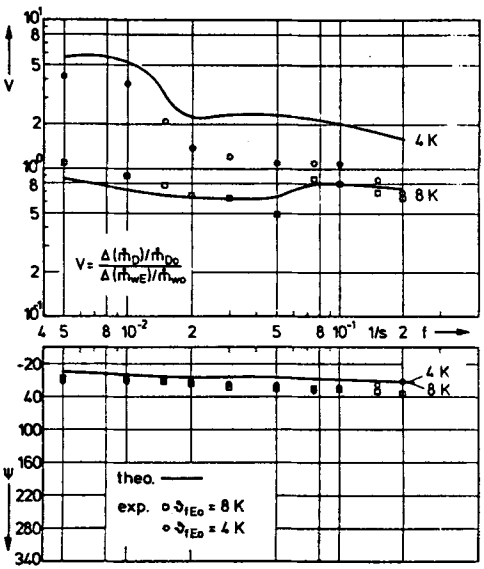

Fig. 15: Amplification factor and phase shift of evaporated refrigerant mass flow rate (measured and calculated). Mass flow rate of condensing vapour perturbated. Constant subcooling

frigerant flow - are regarded. Theory and experiment show a sudden and large change in the amplification factor, as well as in the phase angle for the boiling pressure drop.

To understand physically this behaviour, the wall temperature along the heat exchanger has to be discussed. Temperature readings in the upper-part of the tube wall allow the conclusion, that there temporarily and locally partial film boiling occured. Perturbations of the condensing vapour flow on the water side, not only caused and eliminated this partial film boiling up and down in the tube on the boiling side. These instabilities strongly influenced the transfer functions. At low perturbation frequences partial film boiling could be observed in the upper part of the heat exchanger over the whole oscillation period. With increasing frequency, the response behaviours became more pronounced and strong pulsations in the wall temperature and in the mass flow rate of the refrigerant could be observed. This pulsations can be explained by the fact that high condensing vapour flow rate strongly produces film boiling and in the period of low vapour flow rate bubble boiling can be re-installed again. With very high frequences the secondary side cannot fully follow the primary perturbations due to storage effects in the wall. The mean values of the heat flux density were below critical heat flux and nucleate boiling staid stable in the refrigerant flow which resulted in a stronger amplification of the pressure drop oscillations, due to higher evaporation rates.

In the fig. 10 - 15 the perturbation amplitude in the vapour mass flow rate was the same. In fig. 16 the validity of the theoretical model is illustrated for different perturbation amplitudes. The transfer functions for the mass flow rate of the vapour produced by boiling are in good agreement for high perturbation amplitudes, as well as for low ones.

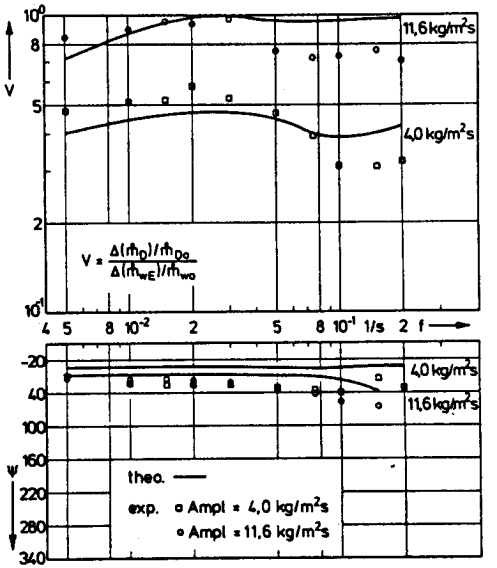

Fig. 16: Amplification factor and phase shift of evaporated refrigerant mass flow rate (measured and calculated). Mass flow rate of condensing vapour perturbated. Constant mixture flow rate.

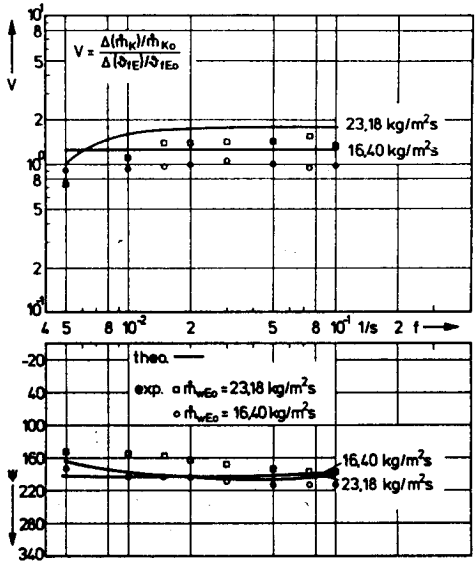

Fig. 17: Amplification factor and phase shift of condensed steam flow rate (measured and calculated) perturbation of inlet temperature on boiling side.

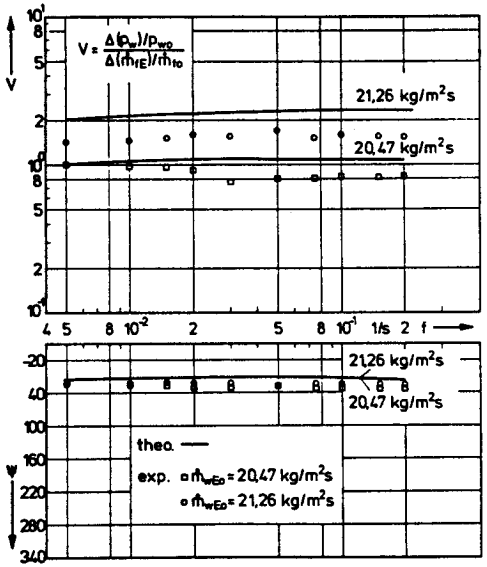

Fig. 18: Amplification factor and phase shift of pressure drop (calculated and measured), perturbated mass flow on boiling side.

4.2 Perturbations On The Secondary Side

With perturbations on the secondary side, the numerical procedure by solving the differential equations in the code becomes a little more complicated, however, the physical models are the same as with perturbations in the condensing steam flow. As demonstrated in the fig. 17 and 18, the system stays more stable with perturbations on the secondary side than on the primary one. The reason for this is very easily to be understood. The heat source on the primary side is a system of constant temperature. If the mass flow rate of the boiling refrigerant is changed - see fig. 17 - the heat transfer coefficient in the boiling region, inclucing the subcooled boiling area, is not to much affected. Only if single phase heat transfer prevails which is the case at higher mass flow rates, the amplification coefficient becomes larger and deviates remarkably from one.

In fig. 18 is shown how fluctuations in the mass flow rate of the refrigerant influence the pressure on the condensing side. With decreasing mass flow rate of the refrigerant, the heat transport is slightly more deteriorated than with increasing mass flow rate. This effect, however, is partially balanced by a prolongation of the subcooled boiling area. To transport the same amount of heat with a somewhat lower heat transfer coefficient a higher temperature difference between primary and secondary side is needed. This is automatically achieved by rising the temperature and via the saturation conditions also the pressure of the condensing steam. So the amplification coefficient for this transfer function is near one.

5. CONCLUSIONS

The computer code predicting the dynamic behaviour of a double phase change heat exchanger is in good agreement with experimental results as long as no fluiddynamic instabilities occur and as the frequency of the fluctuations is not to high. The later restriction is a consequence of the simplified assumptions made in the physical model which neglect the heat storage in the structure material and thermodynamic disequilibrium in the fluids. Instabilities are strongly system dependant and a correct quantitative prediction needs a very detailed modelling of the geometric data of the whole loop.

In the code a number of empirical and semi-empirical correlations is incorporated describing physical phenomena, like pressure drop or heat transfer, which may be strongly dependant from the geometrical conditions too. Therefore by using the code it has to be checked whether these constitutive equations fit the physical effects influencing the dynamic behaviour well enough also for the design under study. For heat exchangers strongly deviating from the design, discussed here a careful literature survey is needed. For an apparatus which is already operating, the easiest way to adjust the correlations and to verify the code, is to do calibration tests under steadystate conditions and to measure the pressure drop and if possible also the heat transfer coefficients in the range of interest.

REFERENCES

1. Shah, R.K., "Transient behaviour of heat exchangers", Proceedings of the Advanced Study Institute on Heat Exchangers, Istanbul 1980

2. Schöne, A., "Das dynamische Verhalten von Wärmetauschern und seine Beschreibung durch Näherungen", Verlag R. Oldenburg, Minden - Wien, 1966

3. Profos, P., "Die Regelung von Dampfanlagen", Springer-Verlag, Berlin/Göttingen/Heidelberg, 1962

4. Isermann, R., "Das regeldynamische Verhalten von Oberhitzern", Fortschritt-Ber. VDI-Z., Reihe 6, Nr. 4, 1965

5. Hasenkopf, O., "Obertragungsverhalten eines Dampferzeugers in Zusammenwirken mit einem gasgekühlten Kernreaktor", Fortschritt-Ber. VDI-Z. Reihe 6, Nr. 36

6. Varcop, L, "Die Dynamik zwangsdurchströmter Verdampfersysteme unter Berücksichtigung von Druckänderungen des Strömungsmediums", Regelungstechnik 15, 1967, S. 4o4/412

7. Proska, F., "Verfahren zur Berechnung der Frequenzgänge von Gleichstrom- und Gegenstromwärmetauschern", Regelungstechnik 10, 1962, S. 206/210 und S. 256/260

8. Bergles, A.E., "Review of Instabilities in Two-Phase Systems", Proceedings of the NATO Advanced Study Institute on Two-Phase Flows and Heat Transfer, Istanbul, Aug. 1976

9. Veziroglu, T.N., Lee, S.S. and Kakac, S., "Fundamentals of Two-Phase Flow Oscillations and Experiments in Single channel Systems", Proceedings of the NATO Advanced Study Institute on Two-Phase Flows and Heat Transfer, Istanbul, Aug. 1976

10. Schult, M., "Untersuchungen zum dynamischen Verhalten von Doppelrohr-wärmetauschern mit doppeltem Phasenwechsel", Dissertation der Universität Hannover, 1979, Institut für Verfahrenstechn.

11. Bucher, B., "Beitrag zum Siedebeginn beim unterkühlten Sieden mit Zwangskonvektion", Dissertation am Institut für Verfahrenstechnik der Universität Hannover, 1979

12. Saha, P., Zuber, N., "Point of Net Vapour Generation and Vapour Void Fraction in Subcooled Boiling", Proceedings of the Heat Transfer Conference, B 4.7, Tokyo 1970

13. Rouhani, S.Z., "Calculation of Void, Volume Fraction in the subcooled and Quality Boiling Regions", Int. J. Heat Mass Transfer, Vol. 13, 1970, pp. 383/393

14. Dix, G.E., "Vapour Void Fractions for Forced Convection with Sub-cooled Boiling at Low Flow Rates", General Electric Report No. NEDO-10491

15. Ünal, H.C., "Determination of the Initial Point of Net Vapour Generation in Flow Boiling Systems", Int.J.Heat Mass Transfer, Vol. 18, 1975, pp. 1095/1099

16. Chisholm, D., "Pressure Gradients Due to Friction during the Flow of Evaporating Two-Phase Mixtures in Smooth Tubes and Channels", Int. J. Heat Mass Transfer, Vol. 16, 1973, pp. 347/358

17. Nabizadeh, H., "Modellgesetze und Parameteruntersuchungen für den volumetrischen Dampfgehalt in einer Zweiphasenströmung", Dissertation am Institut für Verfahrenstechnik der Universität Hann., 1977

18. Zuber, N., Findlay, J.A., "Average Volumetric Concentration in Two-Phase Flow System", J. Heat Transfer, No. 9, 1960, pp. 453/468

19. Hewitt, G.F., Hall-Taylor, N.S., "Annular Two-Phase Flow, Pergamon Press, 1970

20. Kosky, P.G., Staub, F.W., "Local Condensing Heat Transfer Coefficient in the Annular Flow Regime", AIChE Journal, Vol. 17, No. 5, 1971, pp. 1037/1043

21. Ahrens, K.-H., Mayinger, F., "Boiling Heat Transfer in the Transition Region from Bubble Flow to Annular Flow", Proc. Int. Seminar Momentum, Heat & Mass Transfer in Two-Phase Energy and Chemical Systems, I.C.H.M.T. Dubrovnik, Yugoslavia, 1978

22. Lavin, J.G., Young, E.H., "Heat Transfer to Evaporating Refrigerants in Two-Phase Flow", AIChE Journal, Vol. 11, 1965, pp. 1124

23. Belda, W., "Dryoutverzug bei Kühlmittelverlust in Kernreaktoren", Dissertation am Institut für Verfahrenstechnik der TU Hannover, 1975

Table 2

Additional information on fluddynamic parameters, used in tests and calculations, presented in figures 10 - 18:

Fig. 10:	P_{fEo} = 18 bar	P_{wEo} = 0,46 bar
	$\Delta\vartheta_{fEo}$ = 12° C	$\dot{m}_{wo}$ = 18 kg/m^{2}s
		$\Delta(\dot{m}_{wE})$ = 6,5 kg/m^{2}s
Fig. 11:	P_{fEo} = 18 bar	P_{wEo} = 0,46 bar
	$\Delta\vartheta_{fEo}$ = 12° C	$\dot{m}_{wo}$ = 18 kg/m²s
		$\Delta(\dot{m}_{wE})$ = 6,5 kg/m²s
Fig. 12:	P_{fEo} = 18 bar	P_{wEo} = 0,46 bar
	$\Delta\vartheta_{fEo}$ = 12° C	$\dot{m}_{wo}$ = 18 kg/m²s
		$\Delta(\dot{m}_{wE})$ = 6,5 kg/m²s
Fig. 13:	P_{fEo} = 18 bar	P_{wEo} = 0,46 bar
	$\Delta\vartheta_{fEo}$ = 12° C	$\dot{m}_{wo}$ = 18 kg/m²s
		$\Delta(\dot{m}_{wE})$ = 6,5 kg/m²s
Fig. 14:	$\dot{m}_{fo}$ = 1200 kg/m²s	$\dot{m}_{wo}$ = 18,4 kg/m²s
	$\Delta\vartheta_{fEo}$ = 12 K	P_{wEo} = 0,46 bar
		$\Delta(\dot{m}_{wE})$ = 6,5 kg/m²s
Fig. 15:	$\dot{m}_{fo}$ = 1500 kg/ m²s	$\dot{m}_{wo}$ = 18 kg/m²s
	P_{vEo} = 18 bar	P_{wEo} = 0,48 bar
		$\Delta(\dot{m}_{wE})$ = 6,5 kg/m²s
Fig. 16:	$\dot{m}_{fo}$ = 1200 kg/m²s	$\dot{m}_{wo}$ = 18 kg/m²s
	P_{fEo} = 18 bar	P_{wo} = 0,45 bar
	$\Delta\vartheta_{fEo}$ = 12 K	

Continue Table 2:

Fig. 17:	$\dot{m}_{fo}$	= 1200 kg/m²s	$\dot{m}_{wo}$	= 18 kg/m²s
	P_{fEo}	= 18 bar	P_{wo}	= 0,45 bar
	$\Delta\vartheta_{fEo}$	= 12 K		
Fig. 18:	$\dot{m}_{fo}$	= 1200 kg/m²s	P_{wEo}	= 0,48 bar
	P_{fEo}	= 18 bar	$\Delta(\vartheta_{fE})$	=4,0 K
	$\Delta\vartheta_{fEo}$	= 12 K		